Application of Bayesian Neural Network for modeling and prediction of ferrite number in austenitic stainless steel welds

M. Vasudevan, M. Murugananth*, and A.K. Bhaduri
Materials Joining Section
Metallury and Materials Group
Indira Gandhi Centre for Atomic Research
Kalpakkam
*Department of Metallurgy and Materials Science
Cambridge University, UK

Abstract

As neural networks are extremely useful in recognizing patterns in complex data, Bayesian neural network analysis has been followed in the present work to reveal the influence of compositional variations on ferrite content for the austenitic stainless steel base compositions from the available database and to study the significance of individual elements on ferrite content in austenitic stainless steel welds based on the optimized neural network model. Bayesian neural network's predictions are accompanied by error bars and the significance of each input variable is automatically quantified in this type of analysis. Neural network model based on Bayesian framework for ferrite prediction in austenitic stainless steel welds has been developed using the database which was used for generating the WRC - 92 diagram. The Bayesian framework uses a committee of models for generalization rather than a single model. The best model was chosen based on minimum in the test error and maximum in the logarithmic predictive error. The optimized model can be used for predicting the ferrite number in austenitic stainless steel welds with a better accuracy than the constitution diagrams. Using this model , the influence of variations in the individual elements such as carbon, manganese, silicon, chromium, nickel, molybdenum, nitrogen, niobium, titanium, copper, vanadium, and cobalt on the ferrite number in austenitic stainless steel welds has been determined. It was found that the change in ferrite number is a non-linear function of the

1

variation in the concentration of the elements. Elements such as silicon, chromium, nickel, molybdenum, nitrogen, titanium, and vanadium were found to influence the ferrite number more significantly than the rest of the elements in austenitic stainless steel welds. Manganese was found to have less influence on the ferrite number. Titanium was found to influence the ferrite number more significantly than niobium. This observation is new as WRC - 92 diagram only considered the niobium content in calculating the chromium equivalent.

1. 0 Introduction

The ferrite content in stainless steel welds play an important role in determining the fabrication and service performance of welded structures. The ability to estimate the ferrite content accurately has proven very useful in predicting the various properties of stainless steel welds. A minimum ferrite content is necessary to ensure hot cracking resistance in these welds[1-5], while an upper limit on the delta-ferrite content determines the propensity to embrittlement due to secondary phases [6] (e.g., sigma phase) formed during elevated temperature service. At cryogenic temperatures, the toughness of the stainless steel weld is strongly influenced by the ferrite content [7]. In duplex austenitic-ferritic stainless steel weld metals, a lower ferrite limit is specified for stress corrosion cracking resistance while the upper limit is specified to ensure adequate ductility and toughness[4]. Hence, depending on the service requirement a lower limit and/or an upper limit on ferrite content is generally specified. During the selection of filler metals the ferrite content is normally estimated from the constitution diagrams such as the Schaeffler [8], DeLong[9] and WRC–92 diagrams [10]. These constitution diagrams are based on different Cr_{eq} and Ni_{eq} formulae as given in the Table 1. The coefficients for C and Nb have been increased from 30 and 0.5 in the Schaeffler and DeLong diagrams to 35 and 0.7, respectively, in the WRC–92 diagram, whereas for N it has been lowered to 20 from 30 in the DeLong diagram. The WRC – 92 diagram estimates the

ferrite content to reasonably good accuracy and also provides additional information about the mode of solidification. In these diagrams, the ferrite contents of various welds had been measured experimentally by either metallography (Schaeffler) or magnetic methods (DeLong and WRC–92) and are presented as iso-ferrite content maps.

Constitution Diagram	Cr_{eq} and Ni_{eq}
Schaeffler Diagram (1949)	Cr_{eq} = Cr + Mo + 1.5 Si + 0.5 Nb Ni_{eq} = Ni + 30C + 0.5 Mn
DeLong Diagram (1973)	Cr_{eq} = Cr + Mo + 1.5 Si + 0.5 Nb Ni_{eq} = Ni + 30C + 30 N + 0.5 Mn
WRC–92 Diagram (1992)	Cr_{eq} = Cr + Mo + 0.7 Nb Ni_{eq} = Ni + 35C + 20N + 0.25 Cu

Table1: Cr_{eq} and Ni_{eq} formulae used for estimating the delta-ferrite content from constitution diagrams

The ferrite content in stainless steel   weldments is controlled by several factors and is the result of the series of   microstructural changes that take place during the welding process [11]. Thus, the relationship between the alloy composition and the ferrite content can be quite complex. Linear expression such as given in the above equations can not be expected to take into account all the crucial factors. The relative influence of each alloying addition given by that elements coefficients in the Cr_{eq} or Ni $_{eq}$ expression is likely to change when there is a change in the base composition. In addition, constitution diagrams that rely on simple linear expressions for the Cr_{eq} and Ni_{eq} ignore the interactions between the elements. Hence, the ferrite content estimated using the constitution diagrams will always be less accurate and will never be closer to the measured values.

Kotechi [3] has pointed out that there are number of alloying elements that have not been considered in the most accurate diagram to date, the WRC – 92 diagram. Elements like silicon, titanium, tungsten are not given due considerations though they are known to influence the ferrite content. He also stressed the point that cooling rate effects need to be considered more thoroughly in these constitution diagrams.

Recent research activities have been focused on studying the effect of various alloying elements on the ferrite content and controlling ferrite content by modifying the weld metal compositions. In another approach for estimating ferrite content (Function Fit model), the difference in free energy between the ferrite and the austenite was calculated as a function of composition and this was related to ferrite number. The advantages of this semi-empirical model[12] over the WRC 1992 diagram was that the model considers the effect of other alloying elements and the ease of extrapolation of the model to higher Cr_{eq} and Ni_{eq} values. The major limitation of the constitution diagrams in not acounting for the elemental interactions was overcome by the use of neural networks in predicting ferrite content in stainless steel welds by Vitek et al[13-14]. The improvement of accuracy in predicting the ferrite content by the use of neural networks (feed-forward network with a back-propagation optimization scheme) has been clearly brought by their study. The effect of various element additions on the ferrite content for few base compositions was examined by simply calculating the ferrite number as a function of composition. However, it was not possible in their analysis for direct interpretation of the elemental contributions to the final ferrite number.

Other methods and constitution diagrams are continuously being put forward to predict the ferrite content for a wider range of stainless steel types. Thus, Prediction and measurement of ferrite in stainless steel welds remains of scientific interest due to inaccuracies involved in all the current methods. In this context, the development of a more

accurate predictive tools for estimating the effect of various alloying elements on the ferrite content for different stainless steel welds assumes importance.

The neural network analysis can capture interactions between the inputs because the hidden units are nonlinear. The training process involves a search for the optimum non-linear relationship between the inputs and the outputs, and is computer intensive. The outcome of the training is a set of coefficients (called weights) and a specification of the functions which in combination with the weights relate the input to the output. Once the network is trained, estimation of the outputs for any given inputs is very rapid[15].

A potential risk associated with neural network analysis is overfitting of the training data. To avoid overfitting, Mackay[16] has developed a Bayesian framework to control the complexity of the neural network. Main advantages of this method are that it provides meaningful error bars for the model predictions and also it is possible to identify automatically the input   variables which are important in the non-linear regression. This methodology has proved to   be extremely useful in materials science where properties need to be estimated as a function of a vast array of inputs. In the present study, Bayesian neural network analysis has been applied to develop a generalized model for predicting ferrite number using data that were used to generate the WRC – 1992 diagram. Using the generalized model, the effect of individual elements on the ferrite number for two different base compositions has also been quantified. The accuracy of the model has also been compared with the other ferrite number (FN) prediction methods.

2. 0 Database

The data that was used for generating the WRC –1992 diagram have been used in the present analysis. This database consists of stainless steel SMA (submerged metal arc) weld compositions and ferrite contents. The data well represented the common 300 -series stainless steel weld compositions such as 308, 308 L, 309, 309 L, 316, 316 L types. This database was

collected from the literature [4]. The aim of the analysis was to model the ferrite number as a function of chemical composition. The database consists of 924 data lines. For the cases where the composition values were not available for elements such as Nb, Ti, V, Cu and Co the values were assumed zero. Table 2 gives the range, mean and standard deviation of the each composition variable and the output. This simply gives the idea of the range covered and can not be used to define the range of applicability of the neural network model as the input variables are expected to interact in neural network analysis. In Bayesian neural network analysis, size of the error bars define the range of useful applicability of the trained network. Scatter in the data for each input variable is shown in fig. 1.

Table 2 Range, Mean, standard deviation of the each input variable and the output.

Elements	Minimum	Maximum	Mean	Std. Deviation
C	0	0.2	0.04	0.0219
Mn	0.35	12.67	1.88	1.79
Si	0.03	6.46	0.53	0.35
Cr	1.05	32	20.51	2.76
Ni	4.61	33.5	11.31	2.56
Mo	0.01	10.7	1.42	1.64
N	0.01	2.13	0.09	0.14
Nb	0	0.88	0.03	0.098
Ti	0	0.33	0.02	0.028
Cu	0	6.18	0.14	0.437
V	0	0.23	0.04	0.04
Co	0	0.69	0.03	0.046
Fe	45.59	72.51	63.94	4.33
FN	0	98	12.04	17.31

3. 0 Bayesian Neural Network Analysis

The Bayesian neural network analysis has been extensively used for modeling and prediction of mechanical properties in welds[17-20] and alloys[21]. The complete description of the method is

described elsewhere[16]. The aim of the analysis is to model the ferrite number in stainless steel welds as a function of composition. The networks employed consists of thirteen input nodes, x_i, representing the thirteen composition variables, a number of hidden nodes, h_I, and one output y. The schematic structure of the network is shown in fig. 2. The single output represents the ferrite number. Both the input and output variables were normalized within the range ± 0.5 as follows

$$x_N = \frac{x - x_{min}}{x_{max} - x_{min}} - 0.5$$

where x_N is the normalized value of x, which has maximum and minimum values given by x_{max} and x_{min}. Eighty neural network models were created using the data. All the models were trained on a training dataset which consisted of a random selection of half of the data (462) from the whole dataset. The remaining (462) formed the test dataset which was used to see how the model generalizes on unseen data. The models differed in terms of the number of the hidden units and random seeds used to initiate the network. For a given number of hidden units, five different sets of random seeds were used. The number of hidden units varied from 1 to 16 for the 80 different models.

The outputs are calculated from the inputs as follows: linear functions of the inputs, x_j multiplied by the weights w_{ij} are operated on by a hyperbolic tangent transfer function

$$h_i = \tanh\left(\sum_j^N w_{ij}^{(1)} x_j + \theta_i^{(1)} \right)$$

so that each input contributes to every hidden unit where N is the number of input variables. The bias is designated θ and is analogous to the constant that appears in linear regression. The transfer from the hidden units to the output is linear, and is given by

$$y = \sum_i w_i^{(2)} h_i + \theta^{(2)}$$

the output y is therefore a non-linear function of x_j, the function usually selected being the hyperbolic tangent because of its flexibility.

The network is completely described if the number of input nodes, output nodes and the hidden units are known along with all the weights w_{ij} and biases θ_i. These weights are determined by training the network which involves the minimization of an objective function. Bayesian neural network analysis developed by Mackay[16] allows the calculation of error bars representing the uncertainty in the fitting parameters. It is possible to make predictions which have two components in the error bars – one representing the perceived level of noise in the output and the second indicating the uncertainty in fitting the data. This second component which comes from a Bayesian frame work allows the relative probabilities of models of different complexity to be assessed. Further it allows us to obtain quantitative error bars which vary with the position in the input space depending on the uncertainty of fitting the function in that region of space. Instead of calculating a unique set of weights, a probability distribution of weights is used to define the fitting uncertainty. The error bars therefore become large when data are sparse or locally noisy. In this context, a very useful measure is the log predictive error (LPE), because the penalty for making a wild prediction is reduced if that wild prediction is accompanied by appropriately large error bars

$$LPE = \sum_n \frac{1}{2}[(t^{(n)} - y^{(n)})^2 / \sigma_y^{(n)2} + \log(2\pi\sigma_y^n)^{1/2}]$$

Note that larger value of the log predictive er ror implies a better model. In this method it is also possible to identify automatically the input variables which are in fact significant in

influencing the output variable. The input   variables which are less significant are down-weighted in the regression analysis.

3. 1 Characteristics of Bayesian Neural Network Model on Ferrite Number

Characteristics of the model could be seen from the plots shown in fig. 3. The perceived level of noise decreases with the increasing complexity   i.e the increase in the hidden units (fig. 3a). The test error goes through a minimum at five units (fig. 3b) and the log predictive error reaches the maximum at fifteen hidden units (fig. 3c). The error bars throughout the present work represent the fitting uncertainty estimated from the Bayesian framework. It is evident from the plot that there are few outliers in the predicted versus measured ferrite number for the test dataset (fig. 3f). Each of these outliers was found to represent unique data not represented in the training dataset. It is possible that a committee of models can make a more reliable prediction than an individual model. The best models are ranked using the values of the log predictive errors. Committees are then formed by combining the predictions of the best L models, where L = 1,2,3 …; the size of the committee is therefore given by the value of L. A plot of the test error of the committee versus its size gives a minimum which defines the optimum size of the committee as shown in the (fig. 3d). As seen in the figure the test error associated with the best single model is clearly greater than that of any of the committees. The committee with 38 models was found to have an optimum membership with the smallest error. The committee was therefore retrained on the entire dataset and used for predictions. The final comparison between the predicted and measured ferrite number values for the committee of 38 is shown in fig. 4. Details of the 38 members of the optimum committee are given in table. 3.

Model	Hidden units	σ_ν
1	15	0.01942
2	14	0.01594
3	7	0.02572
4	12	0.01406
5	7	0.0249
6	5	0.02847
7	11	0.02038
8	7	0.02305
9	16	0.01859
10	3	0.03037
11	10	0.02542
12	8	0.02445
13	6	0.02685
14	9	0.02083
15	6	0.02542
16	8	0.02517
17	10	0.01971
18	15	0.01831
19	13	0.02106
20	10	0.01967
21	14	0.02354
22	4	0.03123
23	8	0.02424
24	4	0.03127
25	11	0.02151
26	12	0.01855
27	11	0.01777
28	13	0.02039
29	1	0.0411
30	1	0.0411
31	1	0.0411
32	1	0.04109
33	1	0.04106
34	5	0.028
35	9	0.01875
36	9	0.02363
37	4	0.0301
38	8	0.01845

Table 3 Hidden units and σ_ν in optimum Ferrite Number committee model

4.0 Results and Discussions

The comparison between the predicted and measured FN values for the committee of models

is shown in fig. 4a for the complete dataset. There was excellent agreement between the

measured and the predicted FN values. The correlation coefficient was determined to be

0.98025. Fig. 4b shows the comparison between the measured and predicted FN values of

316 LN austenitic stainless steel (our lab data), which was not used in training during model

creation. The absolute error between the measured and predicted FN for entire dataset (25

nos) was less than 2. This error value is better than the error values reported by other methods

for unseen data. The size of the error bars in fig. 4b are large for few of the data indicating

compositions similar to that have not been used in the training. Figure 5 indicates the

significance σ_w of each of the input variable as perceived by the first five best models in

committee. The σ_w value represents the extent to which a particular input explains the

variation in the output, rather like a partial correlation coefficient in linear regression

analysis. The elements   Mn and   Nb are not significant in influencing the ferrite

number. Influence of Mn on the ferrite number is insignificant for 300 series stainless steels

and this is in agreement with the results reported in the literature [22] which says that variation

in Mn concentration (in the range from 1 to 12%) has almost no effect on the deposited ferrite

number. Though Nb which is found to be insignificant in the present study finds a place in

the term for calculating the Cr_{eq} for the WRC – 1992 diagram. Cr and Ni were found to be

the main elements in influencing the ferrite number. This is in agreement with the published

literature on ferrite number in stainless steel welds. The other elements to follow are Mo, N,

V, Ti, Cu, Co, Si, C and Fe in that order. As per our model, these elements influence the

ferrite number significantly. However, some of these elements like V, Ti, Co and Si have not

been included in the terms for calculating Ni_{eq} and Cr_{eq} in the WRC – 1992 diagram.

4.1 Comparison of the accuracy of the present model with existing methods

The error distribution (measured FN – Predicted FN) for the Bayesian neural network model

is shown in fig. 6. It can be seen that the absolute error lies within 2.5 for most of the dataset

used in the training while in the case of FNN-1999 model it was less than 3 for around 80% of the dataset used in training [14]. The error distributions for our model is symmetrical about zero implying that model fits the data well. Also the tail of the error distributions are less compared to the other methods[12,14]. The error distributions are quantified and compared with that of the FNN-1999 model in table 4. For all the cases, Bayesian neural network model is better compared to that of the FNN – 1999 model. Vitek et al [14] have reported that FNN – 1999 model is more accurate compared to WRC – 1992 and the Function fit model. Root mean square error between the measured and the predicted FN values for all the four methods (Bayesian neural network model, FNN – 1999 model, Function Fit model and WRC – 1992 diagram) are compared in the table 5. These error values represent the quantitative measure of the degree to which the various models fit the complete dataset on which they were trained. Bayesian neural network analysis has the lowest error of all the four methods. This model has an improvement of 43% over the FNN-1999 model and 65% over the WRC – 1992 diagram. From the comparisons of the accuracies of the predictions by different methods, it is very clear that Bayesian neural network model presented in this work is the most accurate model for prediction of ferrite number in stainless steel welds.

Bayesian Neural Network model			FNN – 1999 model	
Absolute Error	Number of points	% of Total	Number Of points	% of Total
≤ 1.5	684	74.0%	621	64.6%
≤ 2.5	820	88.7%	764	79.5%
≤ 3.5	864	93.5%	826	86.0%
≤ 4.5	888	96.1%	-	-
≤ 5.5	900	97.4%	-	-
≥ 5.5	20	2.16%	-	-
≥ 9.5	4	0.4%	32	3.3%

Table 4 Comparison of the Errors (experimental – Predicted FN) for the Bayesian Neural network model and the FNN – 1999 model[14] (training database)

Prediction Method	RMS Error
Bayesian Neural Network Model	1.99
FNN – 1999 Back Propagation Neural Network Model[14]	3.5
WRC – 1992[10]	5.8
Function Fit Model[12]	5.6

Table 5 Comparison of the Root Mean Square Errors for complete Training database for different FN prediction methods

4.2 Composition dependent behaviour

The severe limitation of the WRC – 92 diagram is that the coefficients in the terms for Cr_{eq} and Ni_{eq} formulae are constant and hence the influence of an individual element on FN is same irrespective of the change in the base composition. As neural networks can take into account the interaction between the input variables and their influence over the output

variable, it would be interesting to study how the change is base compositions affect FN. This was done with two starting base compositions and then allowing each element to vary over a limited range adjusting Fe concentration accordingly but holding all other element concentrations constant. Table 6 gives the base compositions of the two materials for which the effect of concentration of various elements on the ferrite number has been studied.

Material	C	Mn	Si	Cr	Ni	Mo	N	Nb	Ti	Cu	V	Co	Fe
308 L	0.035	0.8	0.4	20.4	10	0.05	0.06	0.07	0.08	0.14	0.09	0.07	67.805
316 L	0.035	0.8	0.9	19.4	11	2.5	0.06	0.07	0.08	0.24	0.09	0.1	64.725

Table 6 : Chemical composition of the two base materials

4.2.1 Application of the generalized model to 308 L austenitic stainless steel weld

The predicted ferrite number vs the variation in the concentration of the individual elements for 308 L austenitic stainless steel are given in the fig. 7. The variation was found to be non-linear. Some of the elements like C, N and Ni are found to decrease the ferrite number with increasing concentration indicating that they are strong austenite stabilizers. The elements like Cr, Si and V are found increase the ferrite number with increasing concentration indicating that they are strong ferrite stabilizers. The variation in the elements like Mn, Mo, Nb, Cu and Co are found not to influence the ferrite number for this base composition. The surprising effect is found for Ti which shows a varying effect on ferrite number. This observation contradicts the observation by Vitek [14] who reported the role of Ti as a strong ferrite stabilizer but for a different base composition. For the present base composition effect of Ti can be explained as follows: Titanium is expected to tie up with carbon and nitrogen very effectively in forming carbides or carbonitrides only at stoichiometric compositions[23,24]. Other than stoichiometric compositions, titanium is less effective in forming the carbides or carbonitrides. So, the strong austenite stablilizers carbon and nitrogen remain in solid solution

14

reducing the ferrite number of the stainless steel. However, this should be verified experimentally.

4.2.2 Application of the model to 316 L austenitic stainless steel weld

The predicted ferrite number vs the variation in the concentration for the individual elements for 316 L austenitic stainless steel are given in the fig. 8. Variation of ferrite number due to change in concentration of elements was found to be non-linear. In the case of 316 L stainless steel, the elements C, Mn, Ni and N are found to decrease the ferrite number with increasing concentration indicating that they are strong austenite stabilizers. The elements Cr, Si and Mo are found to increase the ferrite number with increasing concentration indicating that they are strong ferrite stabilizers. The elements V, Cu and Co are found to increase the ferrite number slightly and hence they are weak ferrite stabilizers. There is a change in the contribution of the individual elements to FN when the base composition is changed. Thus, the severe limitation of the WRC – 1992 diagram that the Cr_{eq} and Ni_{eq} coefficients do not change as a function of the alloy composition has been overcome by using neural network analysis. The role of Cu in its contribution to ferrite number for this base composition is opposite to its role as projected in the WRC – 1992 diagram. The variation in the concentration of the element Nb was found not to influence the ferrite number. Titanium is agin found to show a varying effect on its influence over the FN. The effect of Ti on FN is stronger compared to that of the 308 L stainless steel weld.

5.0 Conclusions

The generalized model for predicting the ferrite number in stainless steel welds using Bayesian neural network analysis has been developed. The accuracy of the Bayesian neural network model in predicting ferrite number is better compared to the existing FN prediction methods. Significance of the individual elements on FN has been quantified. Elements like manganese and niobium are insignificant in influencing the ferrite number. The study has

15

clearly brought out the fact that individual element contributions to FN vary depending on the base composition and hold a non-linear relationship. The variations in the concentrations of silicon, vanadium and titanium is found to significantly influence the ferrite number for the two base compositions studied. Titanium shows a varying effect for both the base compositions considered in the present study. Based on the present study, it is suggested that Cr_{eq} and Ni_{eq} formulas used in the WRC – 92 diagram has to be analyzed further in terms of the elements considered in order to improve the accuracy of prediction of ferrite number for stainless steel welds.

6.0 Acknowledgements

7.0 References

1. C.D. LUNDIN and C.P.D. CHOU, Hot Cracking Susceptibility of Austenitic Stainless Steel Weld Metals, 1983, WRC Bulletin 289, 1-80.
2. C.D. LUNDIN, W.T. DELONG and D.F. SPOND, Ferrite-Fissuring Relationships in Austenitic Stainless Steel Weld Metals, (1975), **54** (8), 241s-246s.
3. D.J. KOTECHI, Ferrite Determination in Stainless Steel Welds – Advances Since 1974, 1997, Welding Journal **76** (1), 24s-37s.
4. C.N. McCOWAN, T.A. SIEWERT and D.L. OLSON, Stainless Steel Weld Metal: Prediction of Ferrite Content, 1989, WRC Bulletin 342, 1-36.
5. D.L. OLSON, Prediction of Austenite Weld Metal Microstructure and Properties, 1985, Welding Journal **64** (10), 281s-295s.
6. J.M. VITEK and S.A. DAVID, 1986, welding Journal, **65** (4), 106s-111s.
7. E.R. SZUMACHOWSKI and H.F. REID, Cryogenic Toughness of SMA Austenitic Stainless Steel Weld Metals, 1978, Welding Journal, **57** (11), 325s-333s.

8. A. SCHAEFFLER, Constitution Diagram for Stainless Steel Weld Metal, 1949, Metal Progress **56**, 680-680B.

9. W.T. DELONG, Ferrite in Austenitic Weld Metal, Welding Journal, 1974, **53**, 273s-286s.

10. D.J. KOTECHI and D T.A. SIEWERT, WRC – 92 Constitution Diagram for Stainless Steel Weld Metals: a Modification of the WRC – 1988 Diagram, 1992,Welding Journal **71** (5), 171s – 178s.

11. J.M. VITEK and S.A. DAVID, The Effect of Cooling Rate on Ferrite in Type 308 Stainless Steel Weld Metal, 1988, Welding Journal, **67** (5), 95s-102s.

12. S.S. BABU, J.M. VITEK, Y.S.ISKANDER and S.A.DAVID, New Model for Prediction of Ferrite Number in Stainless Steel Welds, Science and Technology of Welding, 1997, **2** (6), 279 – 285.

13. J.M. VITEK, Y.S. ISKANDER and E.M. OBLOW, Improved Ferrite Number Prediction in Stainless Steel Arc Welds using Artificial Neural Networks – Part 1: Neural Network Developemnt, Welding Journal, 2000, **79** (2), 33 – 40.

14. J.M. VITEK, Y.S. ISKANDER and E.M. OBLOW, Improved Ferrite Number Prediction in Stainless Steel Arc Welds using Artificial Neural Networks – Part 2: Neural Network Developemnt, Welding Journal, 2000, **79** (2), 41 – 50.

15. H.K.D.H. BHADESHIA, Neural Networks in Materials Science, ISIJ International, 1999, **39** (10), 966-979.

16. D.J.C. MACKAY: 'Mathematical modeling of weld phenomena 3' , H. Cerjack ed., The Institute of Materials, London, 359-389, 1997.

17. S.H. LALAM, H.K.D.H. BHADESHIA and D.J.C. MACKAY, Estimation of Mechanical Properties of Steel Welds Part 1: Yield and Tensile Strength, Science and Technology of Welding, 2000, **5** (3), 135 – 147.

18. S.H. LALAM, H.K.D.H. BHADESHIA and D.J.C. MACKAY, Estimation of Mechanical Properties of Steel Welds Part 2: Elongation and   Charpy toughness, Science and Technology of Welding, 2000, **5** (3), 149 – 160.

19. H.K.D.H. BHADESHIA, D.J.C. MACKAY and L.E. SVENSSON, Imapct Toughness of C- Mn Steel Arc Welds – Bayesian Neural Network Analysis, Materials Science and Technology, 1995, **11** (10), 1046 –1051.

20. E.A. METZBOWER, J.J.DELOACH, S.H.LALAM and H.K.D.H. BHADESHIA, Neural Network Analysis of Strength and Ductility of Welding Alloys for High

Strength Low Alloy Ship building Steels, Science and Technology of Welding, 2001, **6** (2), 116 – 124.

21. R.J. GRYLLS, Mechanical Properties of a High-Strength Cupronickel Alloy-Bayesian Neural Network Analysis, Materials Science and Engineering 1997, **A234-236**, 267-270.

22. E.R. SZUMACHOWSKI and D.J. KOTECHI, Effect of Manganese on Stainless Steel Weld Metal Ferrite, Welding Journal, 1984, **63** (5), 156s-161s.

23. J. WADSWORTH, J.H. WOODHEAD and SR.KEOWN, The Influence of Stoichiometry Upon Carbide Precipitation, 1976, Metal Science, **10**(1), 342.

24. M. VASUDEVAN, S. VENKADESAN and P.V. SIVAPRASAD, Influence of Ti/(C+6/7N) ratio on the Recrystallization Behaviour of a Cold Worked 15CR-15Ni-2.2Mo-Ti Modified Austenitic Stainless Steel, 1996, **231** (3), 231-241.

8.0 Figure Captions

Fig. 1. Database values of each input variable vs Ferrite Number

Fig. 2. Schematic diagram of the network structure Showing the input nodes, hidden units and the output node

Fig. 3. Characteristics of Ferrite Number model

Fig. 4. Comparison of predicted and measured ferrite number for (a) WRC – 92 database (924) which was used in the training (b) our lab data (25) not used in the training, using optimum committee models

Fig. 5. Perceived significance σ_w values of the first five ferrite number models for each input
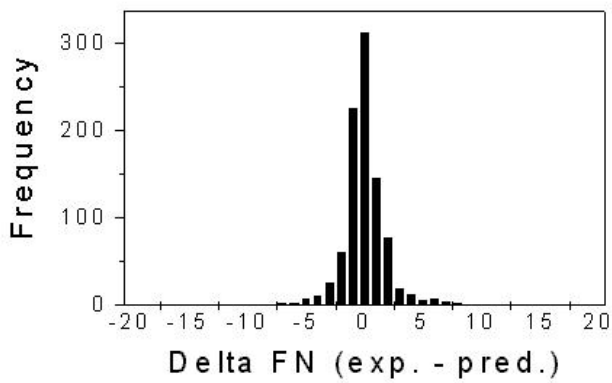
Fig. 6 Error distributions(experimental FN – Predicted FN) for the complete database (924) used in the training

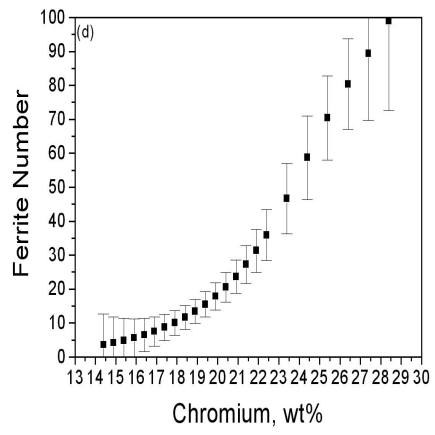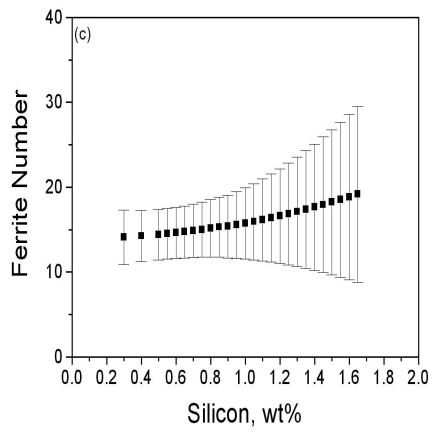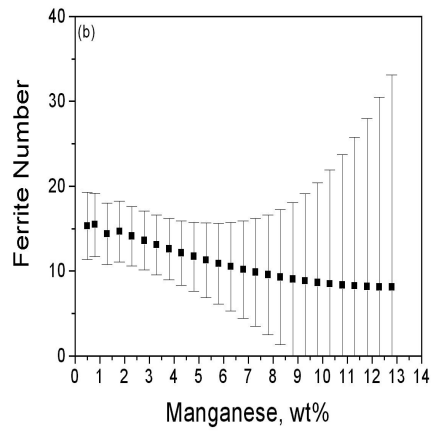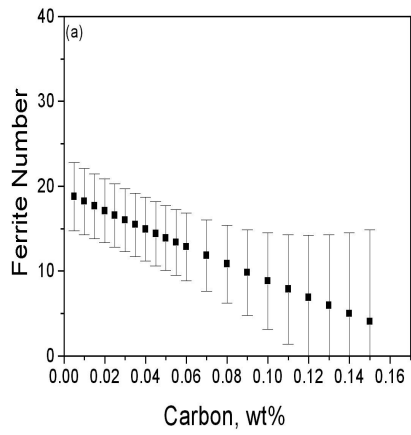Fig. 7. Predicted FN vs concentration of the elements for 308 L austenitic stainless steels weld. The plot shows the variation in the ferrite number when one of the element is varied and all other concentration are held constant at the 308 L composition except Fe, which is adjusted to compensate for the varying element concentration

Fig. 8. Predicted FN vs concentration of the elements for 316 L austenitic stainless steels weld. The plot shows the variation in the ferrite number when one of the element is varied and all other concentration are held constant at the 316 L composition except Fe, which is adjusted to compensate for the varying element concentration

Figures
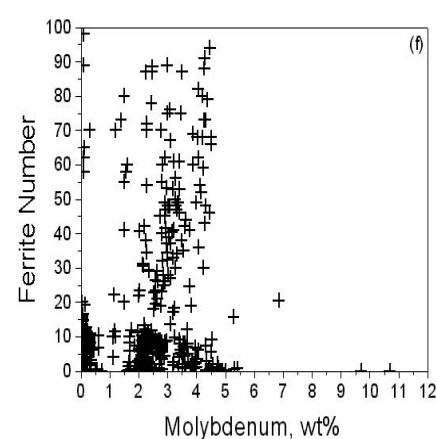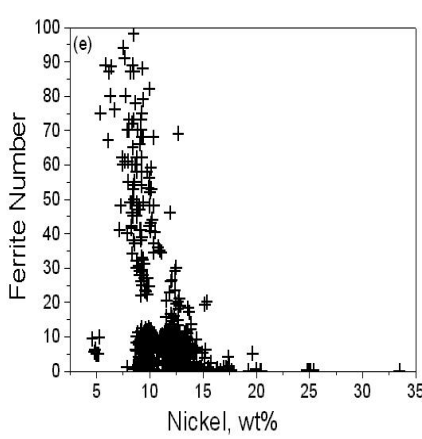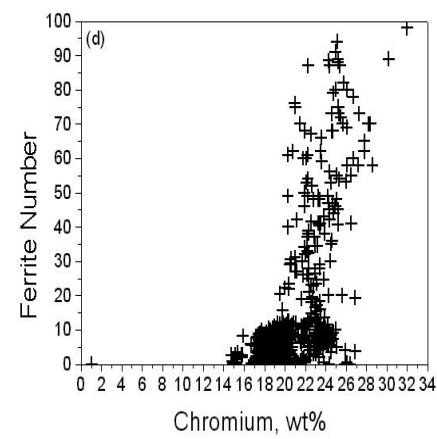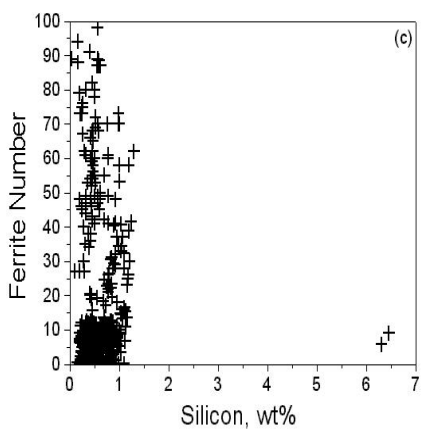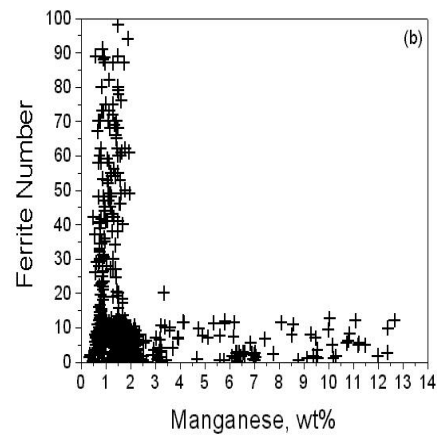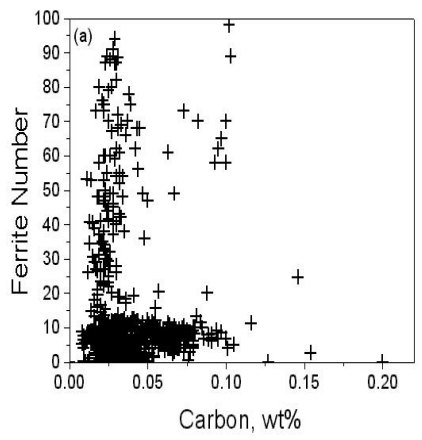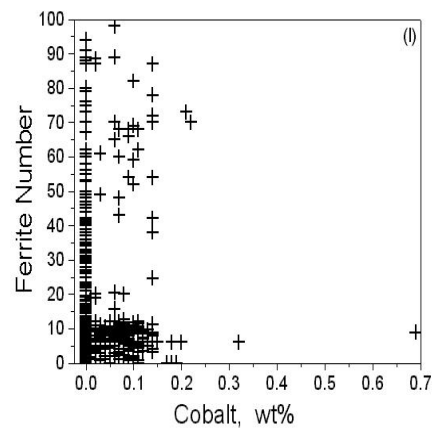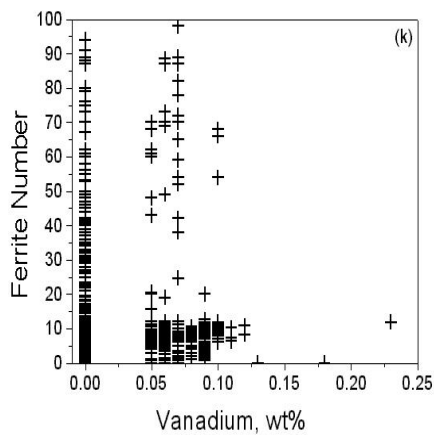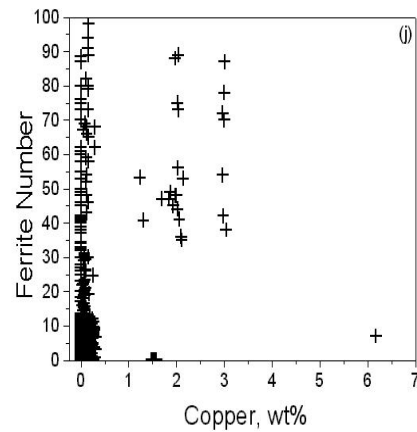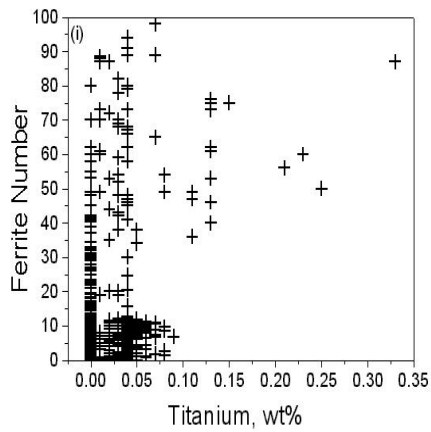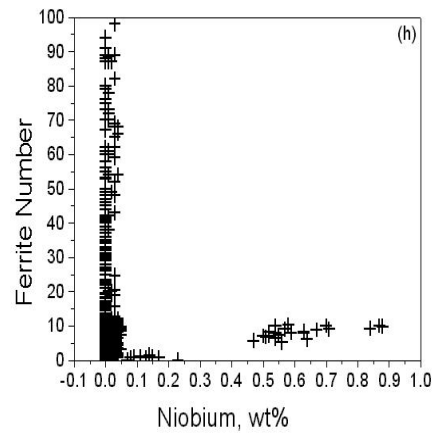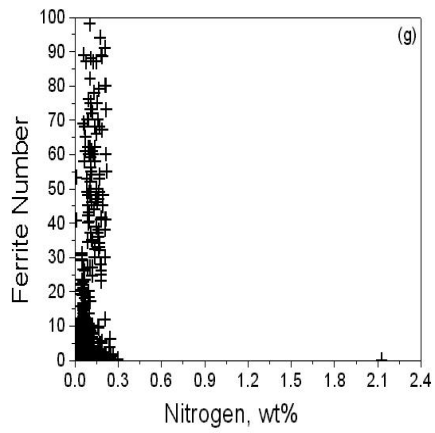
a C; b Mn; c Si; d Cr; e Ni; f Mo; g N; h Nb; i Ti; j Cu; k V; l Co

Fig. 1 Database values of each input variable vs Ferrite Number
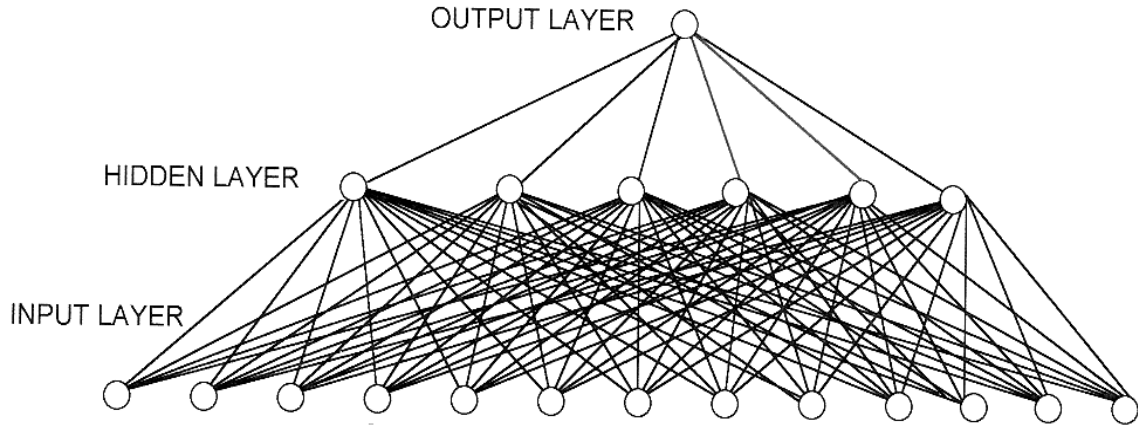
Fig. 2 Schematic diagram of the network structure   Showing the input nodes, hidden
units and the output node
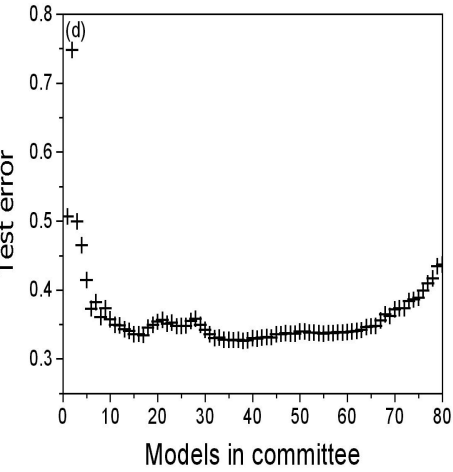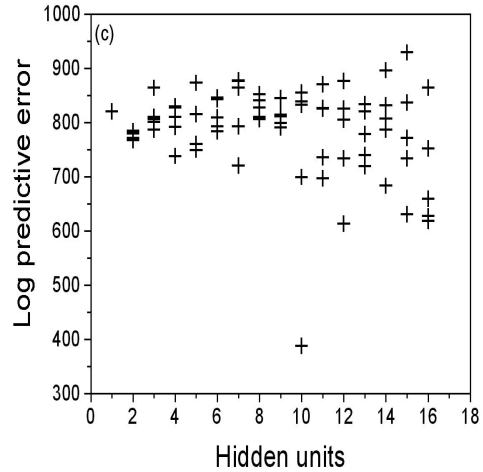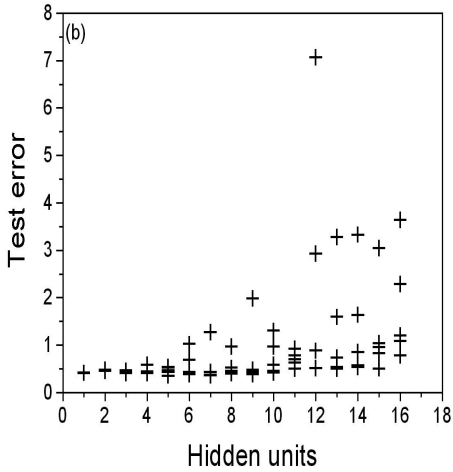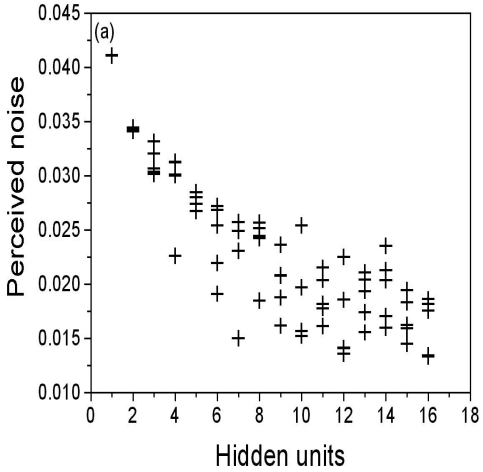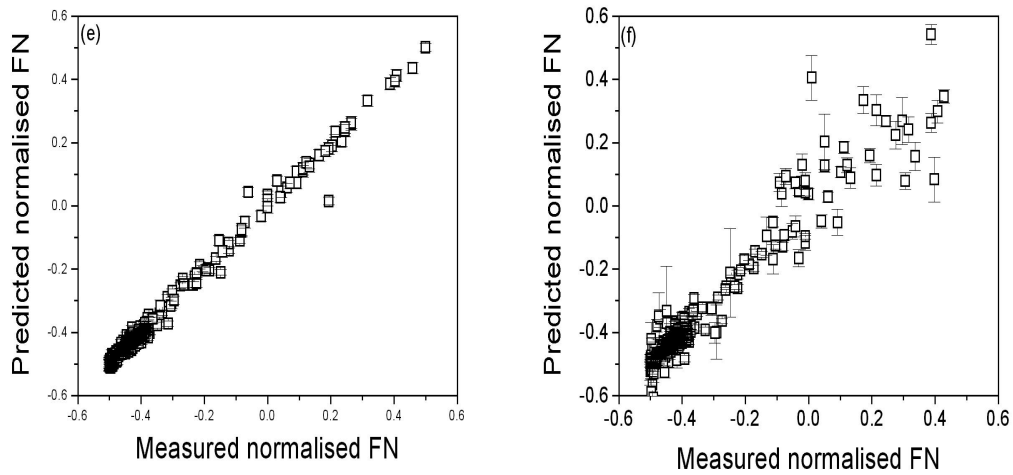
(a) noise vs hidden units ; (b) test error vs hidden units; (c) log predictive error vs hidden units; (d) test error vs models in committee; (e) predicted vs measured FN (training dataset) (f) predicted vs measured FN (test dataset)

Fig. 3 Characteristics of Ferrite Number model
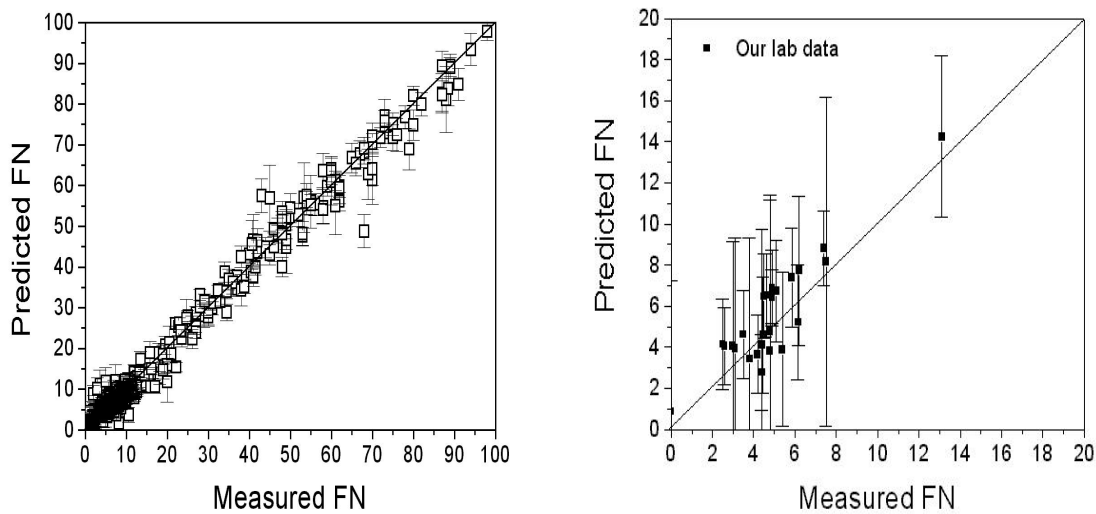
Fig. 4 Comparison of predicted and measured ferrite number for (a) WRC – 92 data base (924) which was used in the training (b) our lab data (25) not used in the training, using optimum committee models
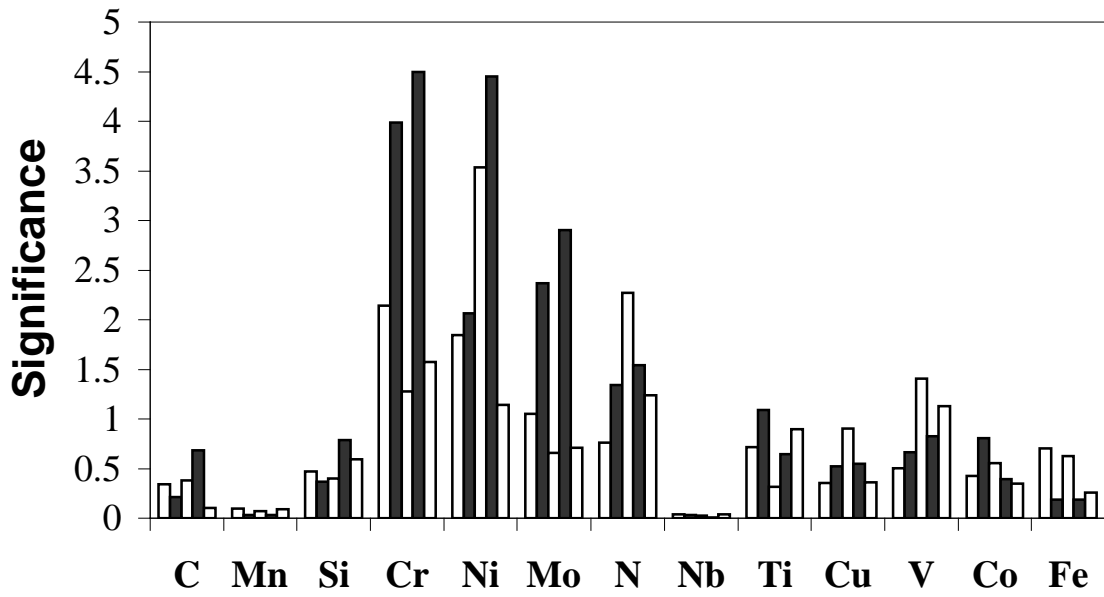
Fig. 5 Perceived significance σ_w values of the first five ferrite number models for each input

Fig.6 Error   distributions(experimental FN – Predicted FN) for the complete database (924) used in the training
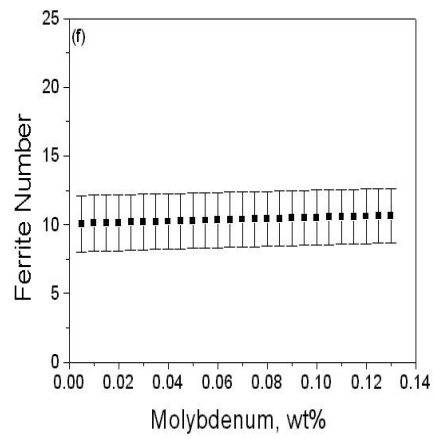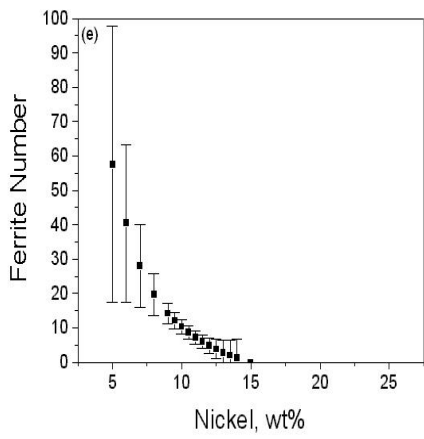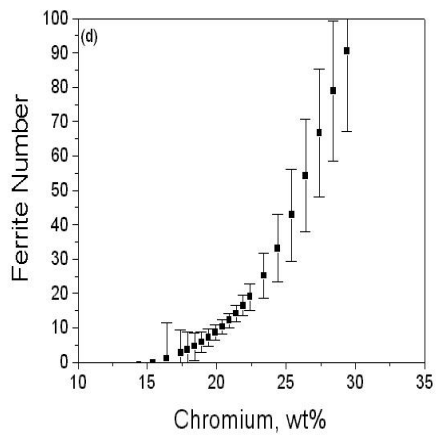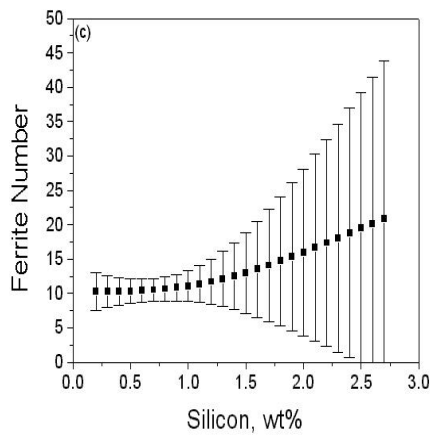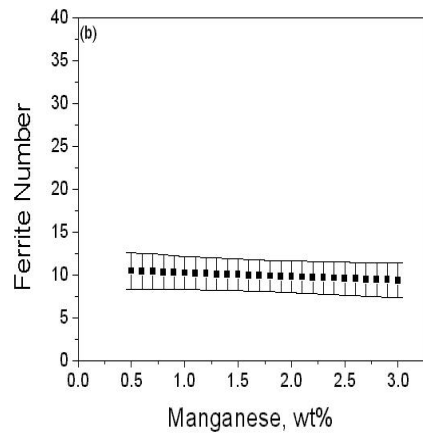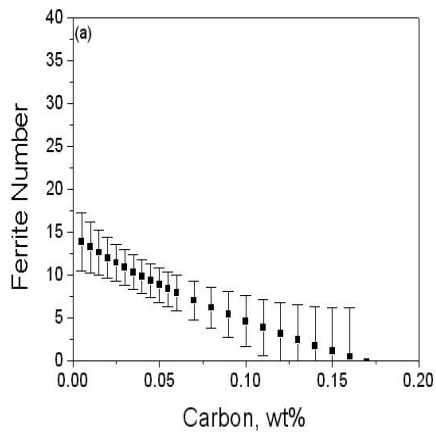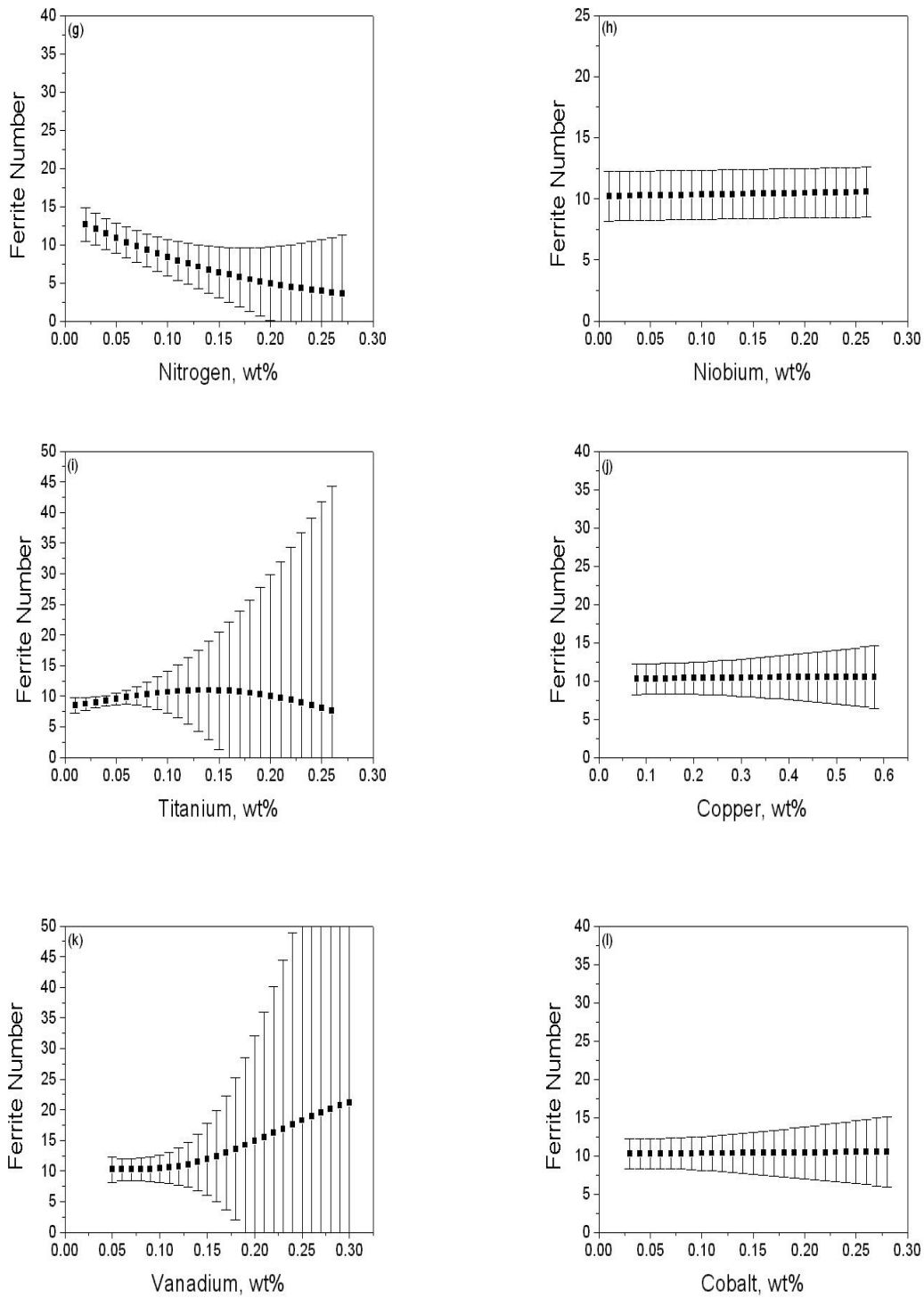
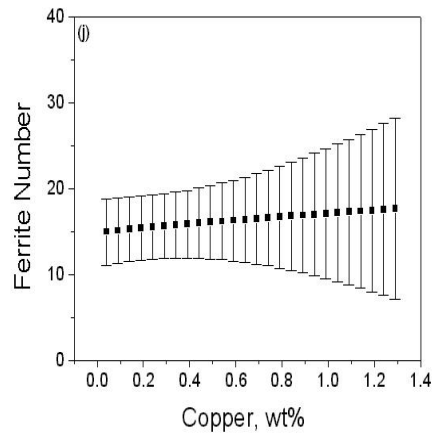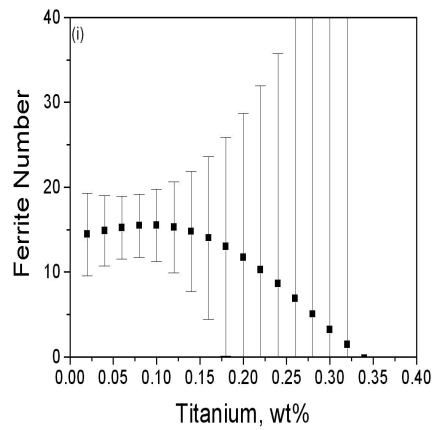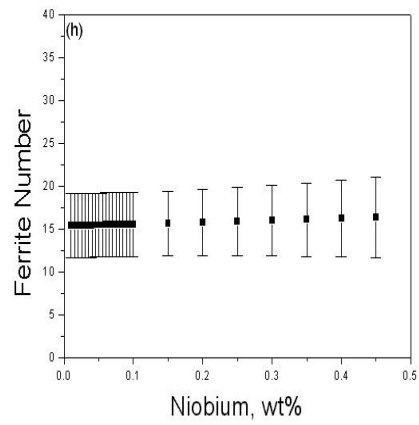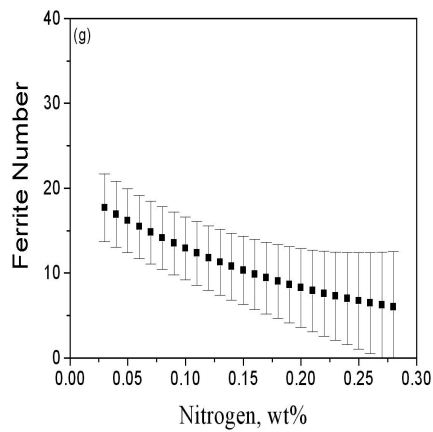a C; b Mn; c Si; d Cr; e Ni; f Mo; g N; h Nb; i Ti; j Cu; k V; l Co

Fig. 7 Predicted FN vs concentration of the elements for 308 L austenitic stainless steels weld. The plot shows the variation in the ferrite number when one of the elements is varied keeping all other concentrations constant for a base composition of 308 L.
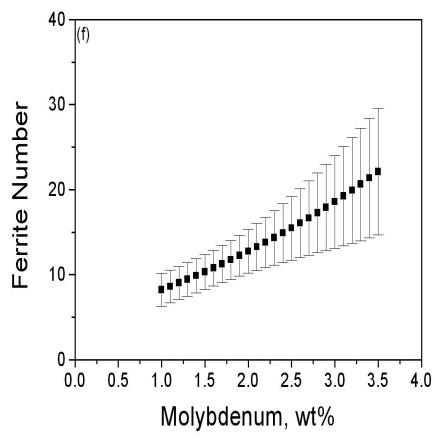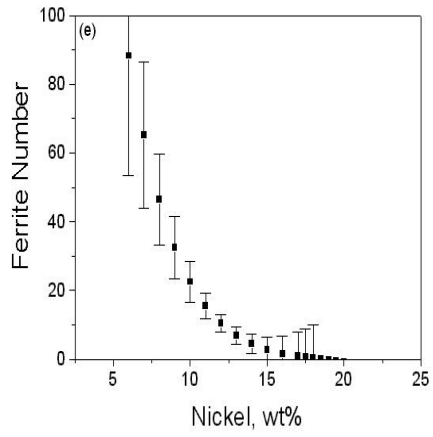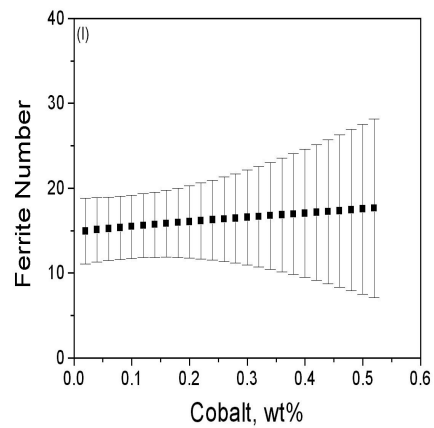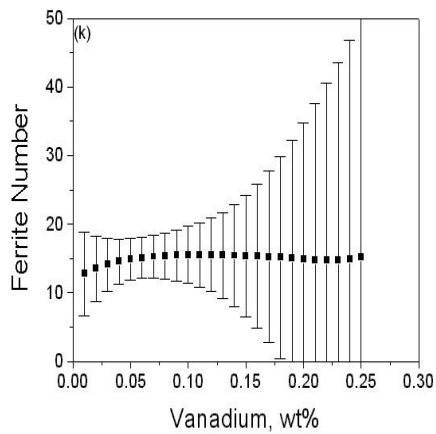
a C; b Mn; c Si; d Cr; e Ni; f Mo; g N; h Nb; i Ti; j Cu; k V; l Co

Fig. 8 Predicted FN vs concentration of the elements for 316 L austenitic stainless steel welds. The plot shows the variation in the ferrite number when one of the elements is varied keeping all other concentrations constant for a base composition of 316 L.